Construction of velocity similarity graph for velocity field analysis in granular intruder motion

Robertas Navakas, Algis Džiugys, Edgaras Misiulis, Gediminas Skarbalius

Lithuanian Energy Institute
Breslaujos g. 3, 44403 Kaunas, Lithuania

Abstract

We present a method based on graph community detection algorithms to analyse velocity fields induced by an intruder particle impinging upon a stationary bed of particles. Based on velocity relations between the pairs of adjacent particles, the "velocity similarity" graphs are built where the graph vertices represent the particles and the edge weights are calculated according to the velocities of the respective particle pairs. A few different expressions for the edge weights are tested. Based on the graph, a Louvain community detection algorithm with the "geographic" null model is used to identify the goups of particles moving in a coordinated manner, represented in the graph as a community of vertices, for which the community detection algorithms developed for graph analysis can be applied. Selection of the expression of the graph edge weights based on the velocities of the respective particles influences the resulting graph structure and thereby has an influence on the community detection results.

1 INTRODUCTION

Mechanical behaviour of granular media is determined by multiple interactions of the constituent particles giving rise to the bulk properties in moving matter. Discrete element simulations (DEM) provide the data of each individual particle i at certain time moments, i.e., the "microscopic" state of the matter, whereas the bulk behaviour, encountered in experiments and practical applications involving granular materials, depends on the large groups of particles arranged in certain structural patterns that can be thought of as a "macroscopic" state. Identification of characteristic larger-scale features of motion of granular media from the particle data is important for understanding the bulk behaviour.

The processes in granular media are based on pairwise particle interactions. These interactions can be represented as a graph where the vertices represent the particles and their interactions as the edges. Earlier, graph theory algorithms were applied for analysis of larger scale structures in granular media [1], as the force chains can be readily represented by graphs. Application of certain

algorithms from graph analysis, such as community detection [2, 3], becomes equivalent to identification of structures in granular media [4, 5, 6]. Analogously, groups of particles moving in a coordinated manner can be identified as graph communities if the edge weights represent the velocity relations [7].

Motion of an "intruder" particle in granular media was analysed from a number of viewpoints [8, 9, 10, 11, 12, 13, 14, 15, 16]. In our case, it is interesting because it provides a characteristic feature of a "shock wave" with rather clear boundary propagating in front of the intruder particle. Detection of this wave can be used as a test of the proposed method. The velocity similarity graph can be constructed using various expressions of the edge weight. We analysed a few expressions to calculate the graph edge weights to construct such a graph from the velocities of the respective particles.

2 SIMULATION METHOD

The considered system consists of a packed bed of 10000 spherical particles partially filling a container (Fig. 1a). The bottom corners of the container are slanted, in order to facilitate the particle motion and thereby prevent excessive mechanical force buildup, in order to avoid possible instabilities during the DEM simulations. The particle radii are random in the range from $r_{\mathrm{min}} = 0.005$ m to $r_{\mathrm{max}} = 0.015$ m. The particle density is $\varrho = 2500$ kg/m^3. Additionally, an extra particle ("intruder") with the radius $r_{\mathrm{int}} = 0.1$ m and density $\varrho_{\mathrm{int}} = 5000$ kg/m^3 is placed at a small height above the packed bed. The initial "intruder" velocity is 10 m/s directed vertically downward. As the intruder reaches the packed bed, the particles therein are put to motion by contact with the intruder (Fig. 1). For easy visualisation, all the particles are fixed in a single plane, but their shapes are considered spherical (a quasi–2D problem). The process was simulated using the `liggghts` software package [17, 18]. In the initial stages, the particles nearest to the intruder start to move and, as the intruder continues its passage, the motion gradually propagates throughout the packed bed and a boundary between the moving and immobile particles appears that can be thought of as a kind of shock wave propagation; even though it is not a rigorous definition, it is a convenient term to refer to the areas of moving particles as opposed to the mostly immobile bulk. Later, the particles in the whole volume of the packed bed start to move and the character of the motion changes. This early propagation of the "shock wave" is a characteristic feature in the granular bed, containing a rather clear-cut single particle group, that can be thought of as a group of particles sharing a certain characteristic parameter (in our case – speed). At later stages of the intruder motion, a canal opens in the wake of the intruder particle (Fig. 1d) that gradually backfills later on (Fig. 1e,f). In these later stages, the character of particle motion is more complex, encompassing a few areas where the nature of motion (direction and speed) varies.

The emergence of particle groups moving faster than the surrounding bulk, i.e., the structure of the velocity field, can be estimated by visualising only the particles moving faster than a certain predefined threshold. Fig. 2 shows

the velocity field (particle velocity vectors) for particles moving faster than a certain fraction of the maximum velocity $|\mathbf{v}|_{\max} \approx 11$ m/s, at the time moment $t = 0.7$ s. A group of particles having velocities $> 0.05|\mathbf{v}|_{\max}$ is visible in front of the advancing intruder particle. The velocity field configuration at this time moment is convenient for analysis, because the single group of moving particles, in contrast to mostly immobile particles located deeper, can be used as a benchmark for easy estimation of detection methods of such groups. At this time, the group still has not reached the walls of the container, therefore, there is no "secondary" motion due to particles bouncing off the walls, and the velocity field has a rather regular structure.

At a later time, after the intruder particle has reached the bottom of the container, the "ballistic canal" starts to fill in. By the same thresholding, a few groups of particles moving bilaterally into the void of the canal can be seen at $t = 3,5$ s (Fig. 3).

3 BUILDING THE VELOCITY RELATIONSHIP GRAPHS

As we represent the similarity of velocities of the nearby particles as the graph edges, the groups of particles having similar velocities can be detected using the mentioned method based on the "velocity similarity" graph.

The graph was built based on the velocities $\mathbf{v}_i$, $\mathbf{v}_j$ of the nearby particles i, j. The particles are considered nearby if $|\mathbf{x}_i - \mathbf{x}_j| \leq f_R\,(r_i + r_j)$, where $\mathbf{x}_i$ and r_i are position and radius, respectively, of particle i. To allow inclusion of particle pairs that are not in direct contact but still close enough from each other, an "extension factor" $f_R = 1.2$ was introduced. The building of the velocity relationship graph is based on defining the graph edge weights depending on the velocities of the respective particles. The particles are considered having "similar" velocity if the angle between their respective velocity vectors is small and the vector lengths are similar. In this case, the values of the scalar (dot) product of the respective vector pairs or the cosine of the angles between these vectors would be high. Moreover, taking into account the speeds of the particles $|\mathbf{v}|$, would enhance the groups of swiftly moving particles against the background of mostly immobile bulk. With these considerations in minds, we used the following expressions for the edge weights:

- similarity of velocities:

$$w_{ij}^{\text{sim}} = 1 - \frac{|\mathbf{v}_i - \mathbf{v}_j|}{\max\limits_{(i,j)\in[1,N_p]} |\mathbf{v}_i - \mathbf{v}_j|}, \tag{1}$$

- velocity difference:

$$w_{ij}^{\text{diff}} = \frac{|\mathbf{v}_i - \mathbf{v}_j|}{\max\limits_{(i,j)\in[1,N_p]} |\mathbf{v}_i - \mathbf{v}_j|}; \tag{2}$$

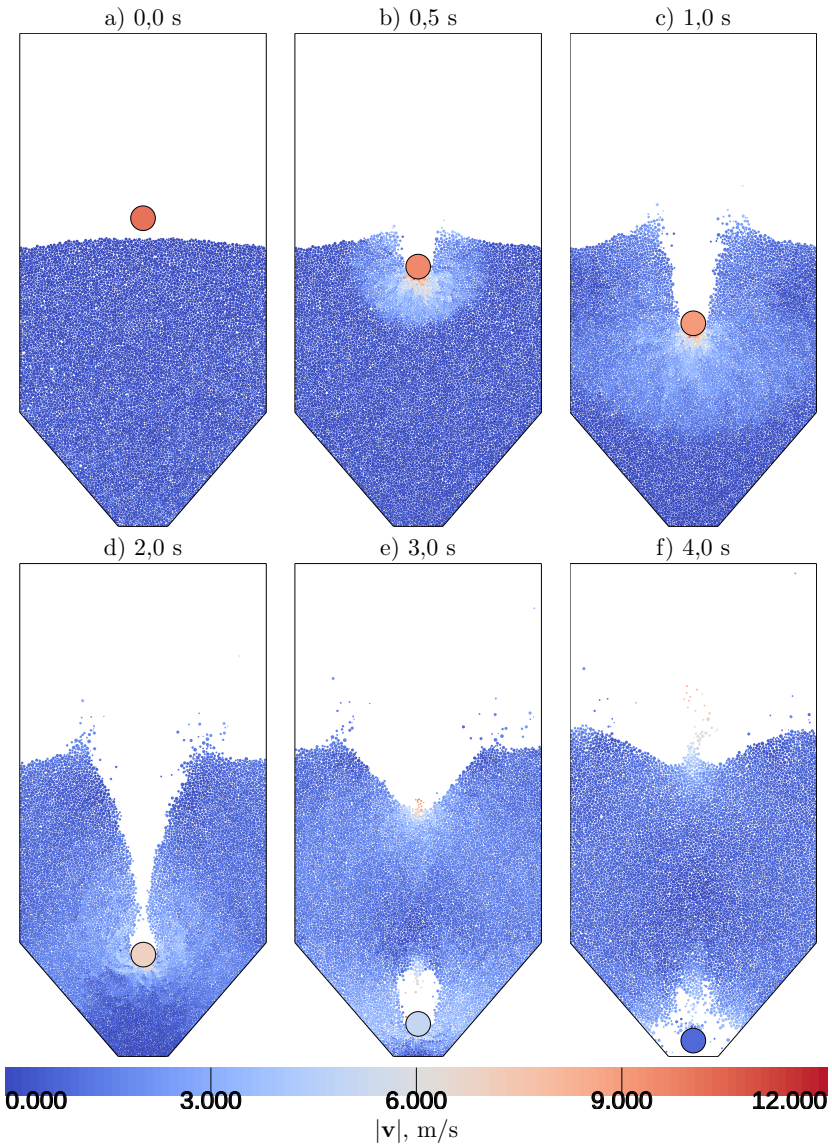

Figure 1: Passage of the intruder at different time moments. The particles are colored according to their speeds (velocity moduli $|\mathbf{v}_i|$).

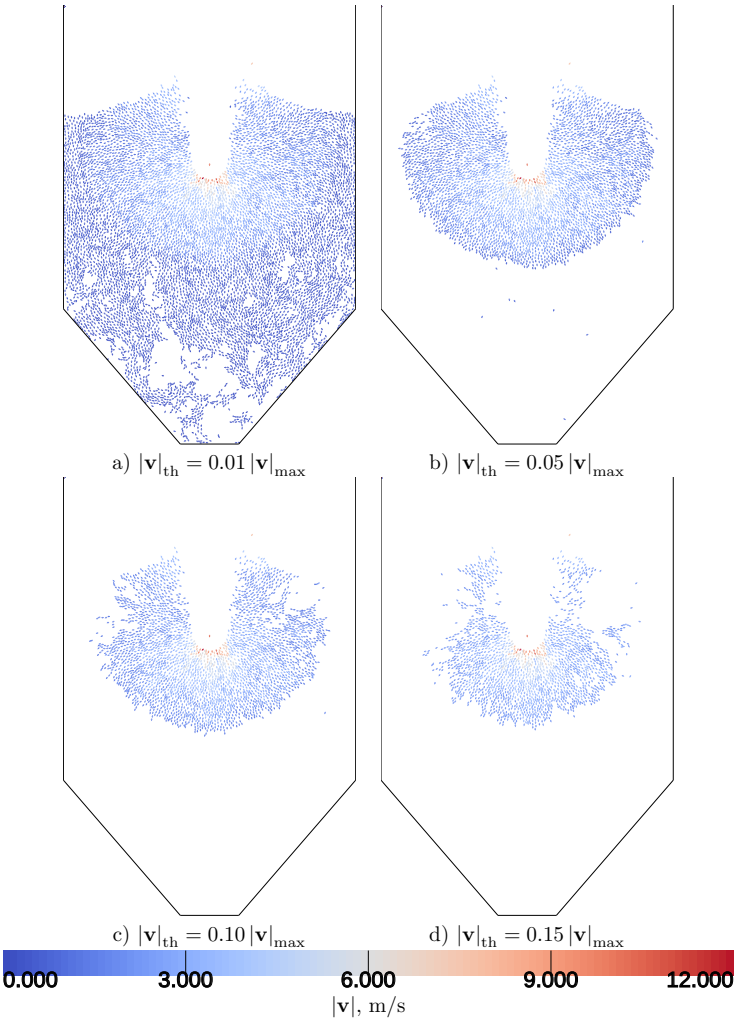

Figure 2: Particle velocities at different speed thresholds at $t = 0.7$ s: only the velocity vectors for particles with speeds larger than the threshold values $|\mathbf{v}|_{\text{th}}$ are shown, with the threshold values of 0.01 (a), 0.05 (b), 0.10 (c) and 0.15 (d) of the maximum speed $|\mathbf{v}|_{\text{max}} \approx 11$ m/s.

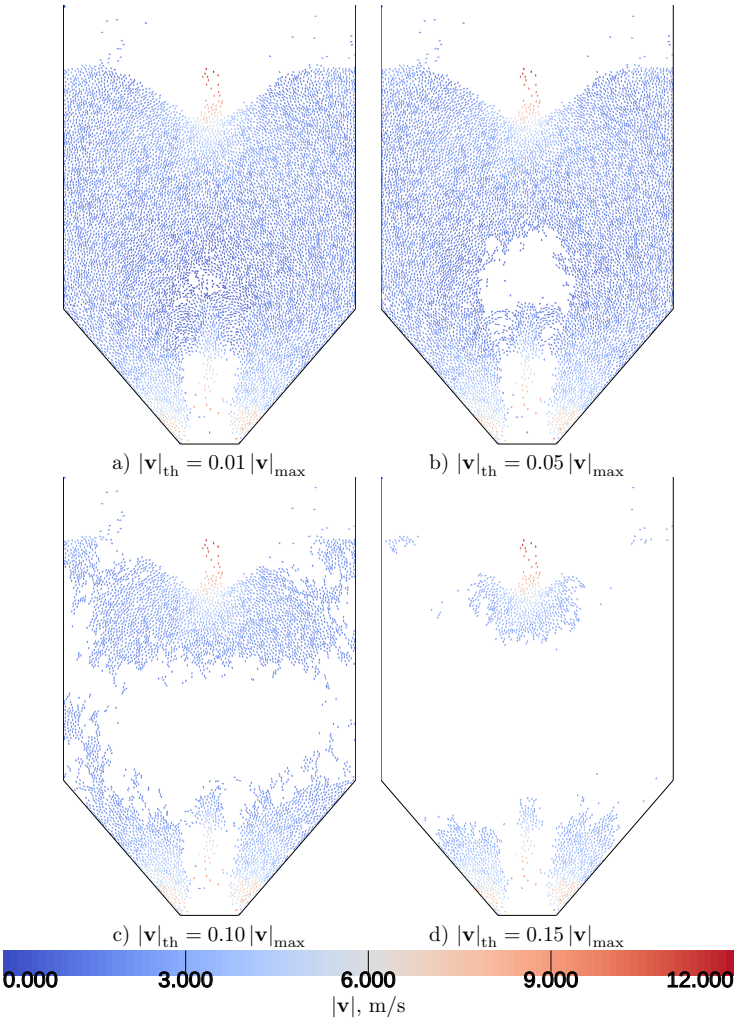

Figure 3: Particle velocities at different speed thresholds at $t = 3,5$ s: only the velocity vectors for particles with speeds larger than the threshold values $|\mathbf{v}|_{\text{th}}$ are shown, with the threshold values of 0.01 (a), 0.05 (b), 0.10 (c) and 0.15 (d) of the maximum speed $|\mathbf{v}|_{\text{max}} \approx 11$ m/s.

in the latter case, the edge weights are larger for the particle pairs with differing velocities. This expression can be used to detect the boundaries between the areas with different character of motion, e.g., the shear zones between the streams with different velocities;

- velocity dot product:

$$w_{ij}^{\mathrm{dot}} = \mathbf{v}_i \cdot \mathbf{v}_j, \tag{3}$$

- normalized velocity dot product:

$$w_{ij}^{\mathrm{dot},v} = \frac{\mathbf{v}_i \cdot \mathbf{v}_j}{\max\left(|\mathbf{v}_i|, |\mathbf{v}_j|\right)}, \tag{4}$$

- cosine of the angle ϕ_{ij} between the velocity vectors $\mathbf{v}_i$, $\mathbf{v}_j$:

$$w_{ij}^{\cos} = \frac{1}{2}\left(1 + \cos\phi_{ij}\right), \tag{5}$$

- normalised cosine of the angle between the velocity vectors:

$$w_{ij}^{\cos,v} = \frac{1}{2}\left(1 + \cos\phi_{ij}\right) \cdot \frac{1}{2}\left(|\mathbf{v}_i| + |\mathbf{v}_j|\right). \tag{6}$$

The expression (5) is based on the assumption that the particles moving in a coordinated manner will move in similar directions, therefore, the cosine of the angle between their velocity vectors would have higher values than that for particles moving in different directions. For convenience of calculations, the expression (5) is normalised to the range $[0, 1]$. This definition does not take into account the speeds of the particle pairs, therefore, it would not discern slower and faster particle groups. To enhance detection of faster particle groups, the expression (6) includes multiplication by the average of the respective particle speeds. Similarly, the pairs of velocity vectors of particles moving in similar directions would produce higher values of the scalar product. On the other hand, dot product of velocities of faster particles moving at more different directions would still produce a larger value of the dot product than that of slow particles moving in less different directions. This effect can be avoided by normalisation to the particle speed (Eq. 4).

As seen above, the time at around $t = 0.7$ s is convenient for analysis because a single rather well- defined structure appears in the velocity field that allows also for visual estimation of the graph structure. The resulting graphs constructed using the expressions (1)–(6) for the time moment $t = 0.7$ s are shown in Fig. 4a–f. In all the graphs, the edge weights w_{ij} were normalised to fit to the range $0 \leq w_{ij} \leq 1$.

The depictions of graphs shown in Fig. 4 are not very revealing visually due to abundance of graph edges, most of which have rather small weights in the area where the particles are not yet put to motion. It is therefore more illustrative to show only the edges having weights exceeding a certain threshold. Fig. 5 shows the edges of the graph, built from the particle velocities at $t = 0.7$ s

using the expression (6), exceeding the values of $0.05w_{\max}$ (a) and $0.15w_{\max}$ (b), where $w_{\max}$ is the maximum edge weight value for this graph. At the low value of threshold $0.05w_{\max}$, a localised structure is already visible that can be estimated as similar to the velocity wave seen in the velocity field (Fig. 2). At higher values of the threshold, this structure is gradually eroded; however, most of the low-weight graph edges corresponding to largely immobile particles can be filtered out.

In comparison, the edge weight expression (Eq. 5) leads to a rather uniform edge weight distribution (Fig. 6). Even at a larger threshold of $0.6w_{\max}$, distribution of the included edges (with $w_{ij} \geq 0.6w_{\max}$) does not reveal any localised structures. This result can be expected, because only the angles between the motion (even slow) directions of nearby particles are taken into account, therefore, the fast moving particles do not stand out in the overall distribution.

On the contrary, the edge weight calculation based on the dot product of the velocity vectors allows for domination of the fastest particle groups (Fig. 7). In comparison to the case of graph edge weights defined using Eq. 6, a rather small particle group emerges. Normalisation to the maximum velocities of the respective particle pairs (Eq. 4) decreases this contrast and the edges distributed throughout the bulk of the particle bed remain present even at a larger threshold of $0.6w_{\max}$ (Fig. 8).

4 RESULTS AND DISCUSSION

Having built the appropriate graph, the standard community detection algorithms known from the graph analysis can be applied [2, 3]. A notable difference between the general community detection approach and that applicable to the graphs built specifically for analysis of granular systems is the choice of null-model: the general algorithms assume that every vertex in the graph has an equal probability to be connected to any other vertex in the null-model. In the granular interaction graphs, where the vertices represent granular particles, this assumption does not hold: only the nearest particles can be in contact, and this constraint should hold also for the representative graph. For this purpose, a "geographic" null model was proposed accounting for this constraint [19, 6]. We used the Louvain algorithm [20] for community detection. The implementation was based on publicly available MATLAB script [21], but we modified it to use the "geographic" null model and to work with GNU Octave. The exhaustive analysis of all the edge weight expressions for building the velocity graph and the resulting community detection results is outside the scope of the present contribution; rather, we focused on the edge weight expression defined by Eq. 6, because it was expected to give the best results based on the above considerations, and this was confirmed by the initial trials.

The community detected in this velocity graph at the time moment $t = 0.7$ s is shown in Fig. 9 as a green outline; the contour of this particle group is obtained by connecting the centers of the outermost particles in the group. For comparison, the outline is superimposed on the velocity fields shown at the

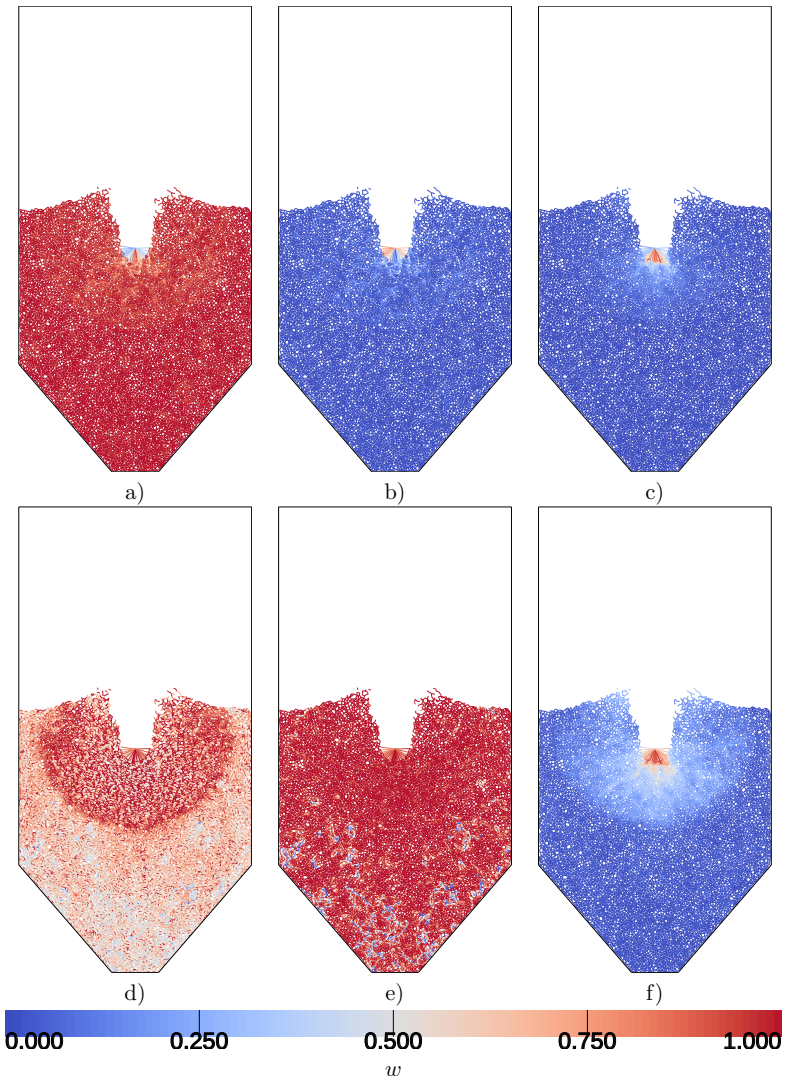

Figure 4: Edges of graphs of velocity relations during the intruder passage at $t = 0.7$ s using the different expressions for graph edge weights: a) $w_{ij}^{\mathrm{sim}} = 1 - \dfrac{|\mathbf{v}_i - \mathbf{v}_j|}{\max\limits_{(i,j)\in[1,N_p]} |\mathbf{v}_i - \mathbf{v}_j|}$ b) $w_{ij}^{\mathrm{diff}} = \dfrac{|\mathbf{v}_i - \mathbf{v}_j|}{\max\limits_{(i,j)\in[1,N_p]} |\mathbf{v}_i - \mathbf{v}_j|}$, c) $w_{ij}^{\mathrm{dot}} = \mathbf{v}_i \cdot \mathbf{v}_j$, d) $w_{ij}^{\mathrm{dot},v} = \dfrac{\mathbf{v}_i \cdot \mathbf{v}_j}{\max\left(|\mathbf{v}_i|, |\mathbf{v}_j|\right)}$, e) $w_{ij}^{\cos} = \dfrac{1}{2}\left(1 + \cos\phi\right)$, f) $w_{ij}^{\cos,v} = \dfrac{1}{2}\left(1 + \cos\phi\right) \cdot \dfrac{1}{2}\left(|\mathbf{v}_i| + |\mathbf{v}_j|\right)$. The graph edges are colored according to edge weights.

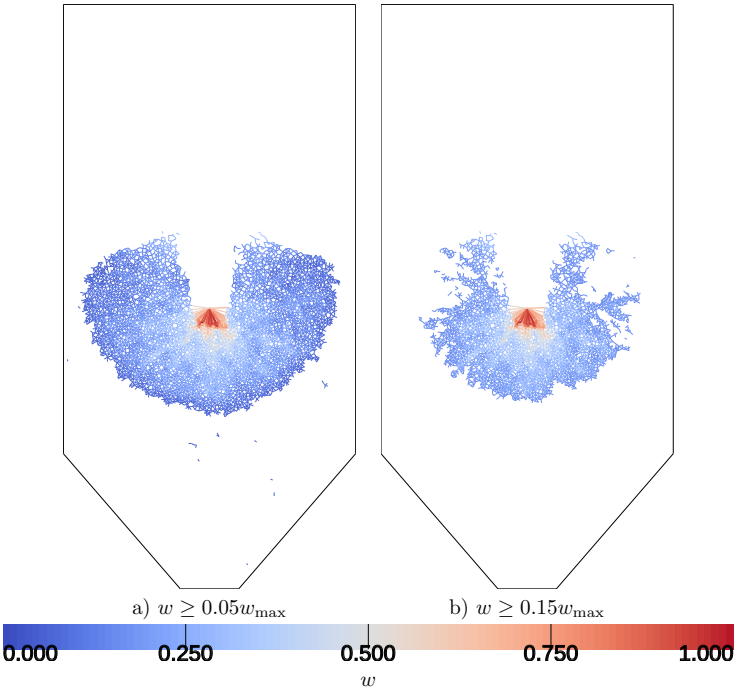

Figure 5: Velocity relations graph built using the expression $w_{ij}^{\cos,v} = \frac{1}{2}(1+\cos\phi) \cdot \frac{1}{2}(|\mathbf{v}_i| + |\mathbf{v}_j|)$ (Eq. 6) for edge weight, with only the edges exceeding the weight threshold shown: at edge weight 0.05 (a) and 0.15 (b) from the maximum edge weight value.

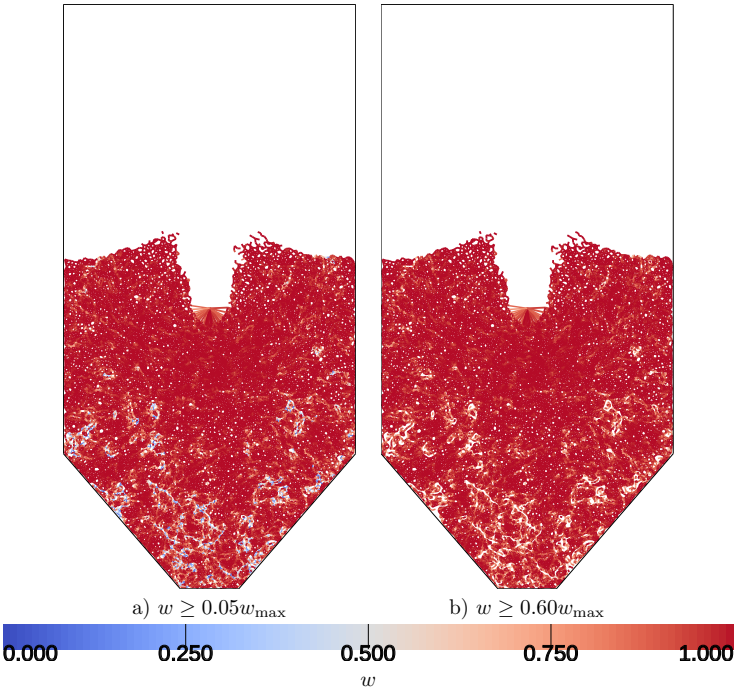

Figure 6: Velocity relations graph built using the expression $w_{ij}^{\cos,v} = \frac{1}{2}(1 + \cos\phi)$ (Eq. 5) for edge weight, with only the edges exceeding the weight threshold shown: at edge weight 0.05 (a) and 0.60 (b) from the maximum edge weight value.

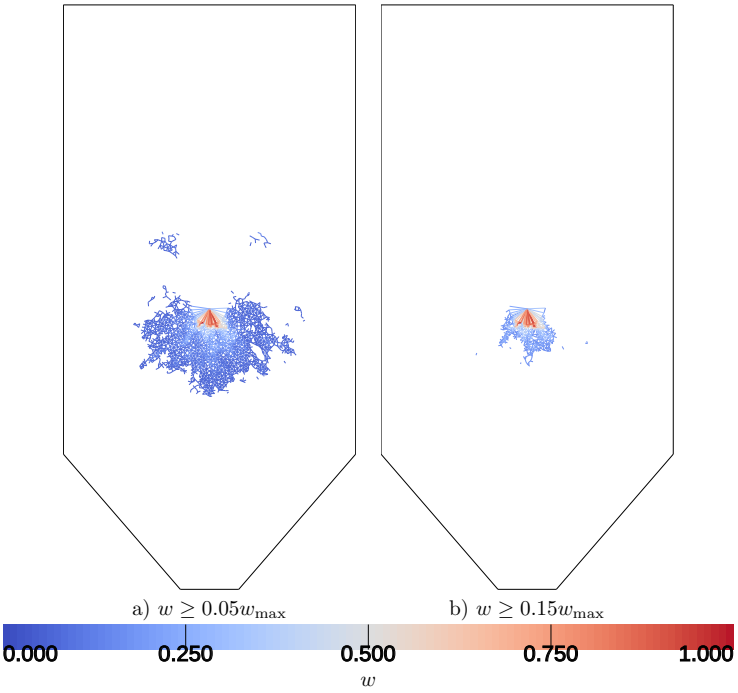

Figure 7: Velocity relations graph built using the expression $w_{ij}^{\text{dot}} = \mathbf{v}_i \cdot \mathbf{v}_j$, (Eq. 3) for edge weight, with only the edges exceeding the weight threshold shown: at edge weight 0.05 (a) and 0.15 (b) from the maximum edge weight value.

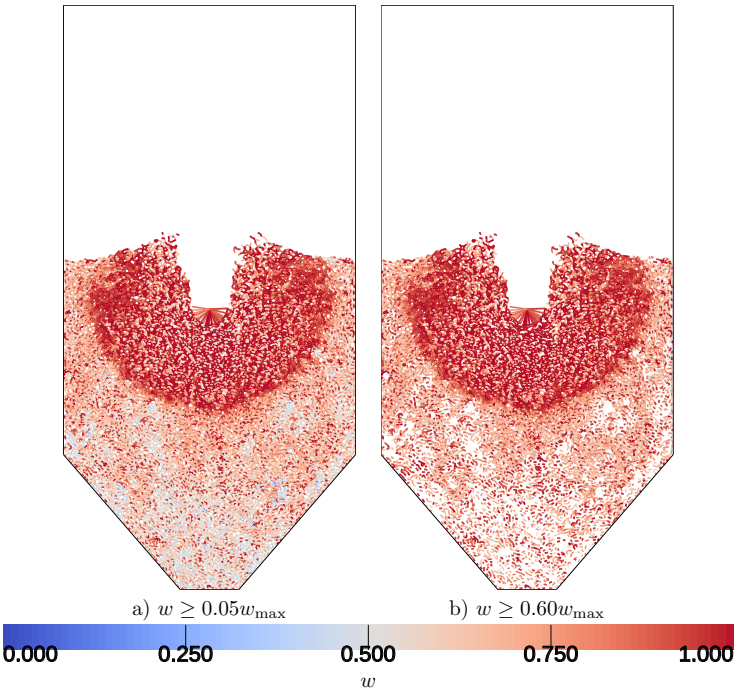

Figure 8: Velocity relations graph built using the expression $w_{ij}^{\mathrm{dot},v} = \frac{\mathbf{v}_i \cdot \mathbf{v}_j}{\max\left(|\mathbf{v}_i|, |\mathbf{v}_j|\right)}$, (Eq. 4) for edge weight, with only the edges exceeding the weight threshold shown: at edge weight 0.05 (a) and 0.60 (b) from the maximum edge weight value.

selected speed thresholds, as in Fig. 2. The largest detected particle group (community) corresponds to the "shock wave" emerging in front of the advancing intruder that can be also detected by simple thresholding. The similarity between the areas of predominant particle motion, as identified by introducing speed thresholds, and the groups of particles detected by the community detection algorithms in the respective velocity graph is also seen in more complex velocity field configurations at the later stages of the intruder motion, such as at the time moment $t = 3.5$ s (Fig. 10). In order to quantify the similarity between the particle groups detected by the community detection algorithm and by setting the speed thresholds, all the particles with speeds above the selected threshold are considered the same community. For partitions produced by the community detection algorithm, all the particles belonging to communities containing more than 5 particles are also considered the same community. This is an approximation in case of partitions containing multiple particle groups, as it is in the case of the partition at $t = 3.5$ s shown in Fig. 10, but it is used to ensure the correspondence to the "partition" obtained by setting thresholds, where assigning the particles to particular groups is complicated. The partitions obtained by setting thresholds and by community detection are then compared using the Jaccard similarity index [22]:

$$J\left(P_c, P_d\right) = \frac{|S_c \cap S_d|}{|S_c \cup S_d|}, \tag{7}$$

where S_c is a set of the graph vertex pairs that belong to the same community in partition P_c, i.e., $(i, j) \in S_c$ if $m_i = m_j$, (i, j) is the pair of vertices i, j, and m_i is the number of community to which the vertex i belongs in the given partition. The calculated indices for time moments 0.7 s and 3.5 s and different threshold ratios f_{th}, such that the particles with $\mathbf{v} \geq f_{\mathrm{th}} \left|\mathbf{v}\right|_{\mathrm{max}}$ are selected, are shown in Table 1. As expected, the highest value of the Jaccard similarity index is obtained in case of a simple velocity field structure containing a single group of moving particles. The similarity between the particle groups obtained by thresholding and community detection methods is lower in case of complex field structures. One of the reasons for this discrepancy is the limited capability of identifying the complex velocity field structures by setting simple thresholds as it was done in the case analysed here. The community detection-based approach can be a more insightful tool for this type of analyses.

Analogously to the cases of the time moments analysed above, the evolution of the group structure of the velocity fields at other time moments is shown in Fig. 11.

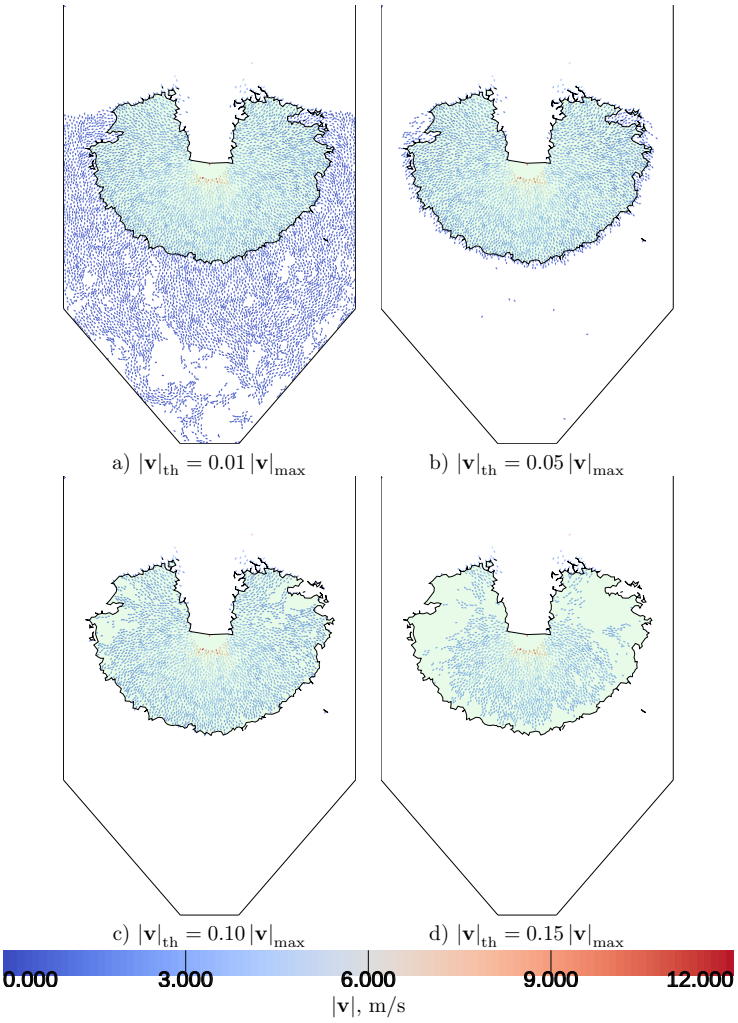

Figure 9: Communities detected from the graph with the edge weight defined as $w_{ij}^{\cos,v} = \dfrac{1}{2}\left(1+\cos\phi\right) \cdot \dfrac{1}{2}\left(|\mathbf{v}_i| + |\mathbf{v}_j|\right)$ (Eq. 6), shown as green outlines, superimposed on the velocity fields at different speed thresholds at $t = 0.7$ s (cf. Fig. 2).

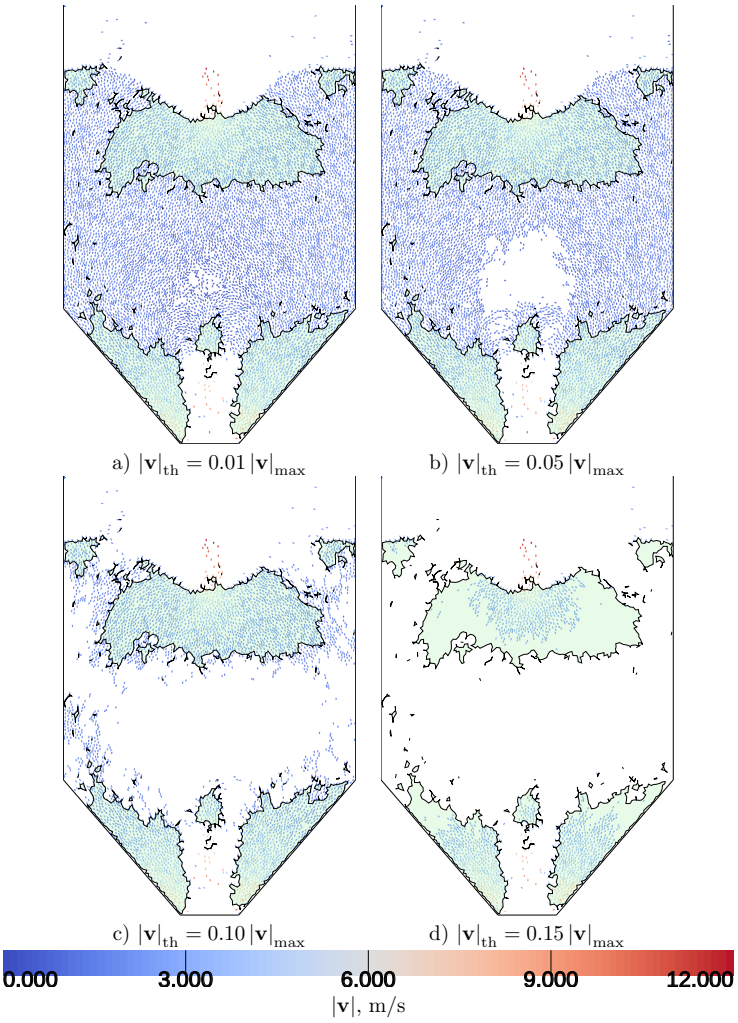

Figure 10: Communities detected from the graph with the edge weight defined as $w_{ij}^{\cos,v} = \frac{1}{2}\left(1+\cos\phi\right) \cdot \frac{1}{2}\left(|\mathbf{v}_i| + |\mathbf{v}_j|\right)$ (Eq. 6), shown as green outlines, superimposed on the velocity fields at different speed thresholds at $t = 3.5$ s (cf. Fig. 3).

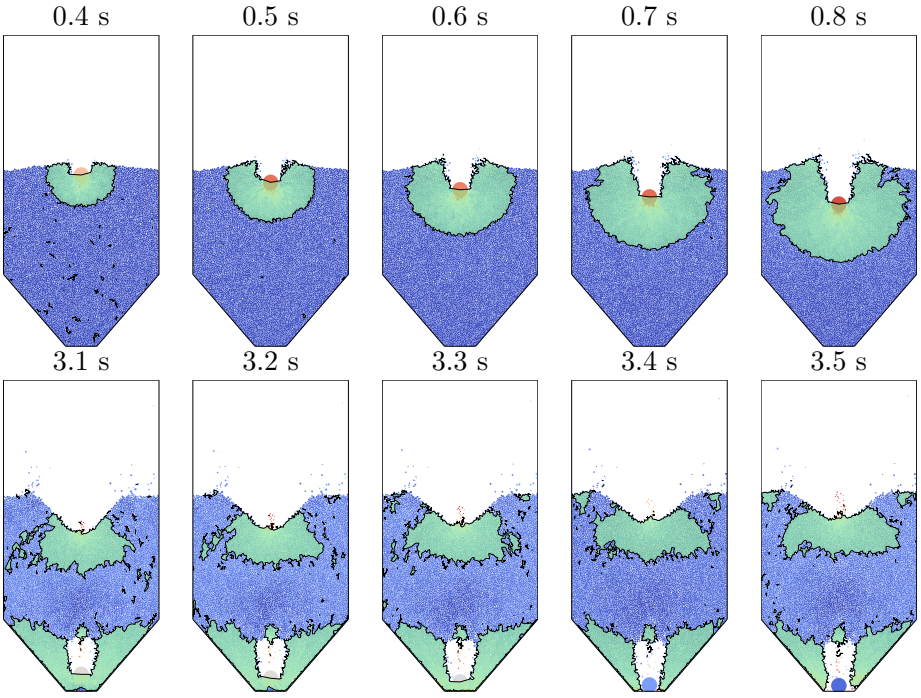

Figure 11: Communities detected using the Louvain algorithm with the "geographic" null model, shown as green outlines, at different stages of the "intruder" passage. The underlying velocity relations graph was build with the edge weights $w_{ij}^{\cos,v} = \frac{1}{2}(1+\cos\phi)\cdot\frac{1}{2}(|\mathbf{v}_i|+|\mathbf{v}_j|)$ (Eq. 6). Only communities containing more than 2 particles are shown.

Table 1: Jaccard similarity indices between the partitions detected using the community detection algorithm and those identified by the particle speed thresholds, at time moments 0.7 s and 3.5 s.

f_{th}	$t = 0.7$ s	$t = 3.5$ s
0.01	0.447	0.533
0.05	0.893	0.479
0.10	0.821	0.647
0.15	0.639	0.579

5 CONCLUSIONS

We have presented an approach for identification of structures in the granular velocity fields consisting of groups of particles moving in a coordinated matter, based on the graph community detection algorithm. For this purpose, a graph is built with edge weights calculated based on velocity relationships between the adjacent particle pairs. The choice of a particular expression for calculation of the graph edge weights has a considerable influence to the resulting graph structure and consequently influences the results of the community detection. In the presented case, an expression for the graph edge weight based on the cosine of the angle between the velocity vectors of the respective particle pairs, taking into account their velocities, turned out to be best suited for our purposes. In many cases, it enables to identify the velocity field structures with high precision.

6 ACKNOWLEDGMENTS

This research was funded by the Research Council of Lithuania under the project P-MIP-17-108 "ComDetect" (Agreement No. S-MIP-17-69), 2017–2020.

7 CONFLICTS OF INTEREST

This work does not have any conflicts of interest.

References

[1] Lia Papadopoulos, Mason A Porter, Karen E Daniels, and Danielle S Bassett. Network analysis of particles and grains. *Journal of Complex Networks*, 6(4):485–565, 2018.

[2] Santo Fortunato. Community detection in graphs. *Physics Reports*, 486:75 – 174, 2010.

[3] Santo Fortunato and Darko Hric. Community detection in networks: A user guide. *Physics Reports*, 659:1–44, 2016.

[4] Robertas Navakas, Algis Džiugys, and Bernhard Peters. Application of graph community detection algorithms for identification of force clusters in squeezed granular packs. In P. Vainiūnas and E.K. Zavadskas, editors, *The 10th International conference "Modern building materials, structures and techniques": selected papers Vol. II*, pages 980–983, Vilnius, Lithuania, May 19–21 2010. Vilnius Gediminas Technical University.

[5] Robertas Navakas, Algis Džiugys, and Bernhard Peters. A community-detection based approach to identification of inhomogeneities in granular matter. *Physica A*, 407:312–331, 2014.

[6] Danielle S. Bassett, Eli T. Owens, Mason A. Porter, M. Lisa Manning, and Karen E. Daniels. Extraction of force-chain network architecture in granular materials using community detection. *Soft Matter*, 11:2731–2744, 2015. arXiv:1408.3841v1 [cond-mat.soft].

[7] Robertas Navakas, Algis Džiugys, Edgaras Misiulis, and Gediminas Skarbalius. Identification of collective particle motion in a rotating drum using a graph community detection algorithm. *Mathematical Methods in the Applied Sciences*, 45(15):8864–8875, 2022.

[8] Abram H. Clark, Alec J. Petersen, Lou Kondic, and Robert P. Behringer. Nonlinear force propagation during granular impact. *Phys. Rev. E*, 114:144502, Apr 2015.

[9] Abram H. Clark, Lou Kondic, and Robert P. Behringer. Steady flow dynamics during granular impact. *Phys. Rev. E*, 93:050901, May 2016.

[10] Hesam Askari and Ken Kamrin. Intrusion rheology in grains and other flowable materials. *Nature Materials*, 15(12):1274–1279, Dec 2016.

[11] A. Seguin, C. Coulais, F. Martinez, Y. Bertho, and P. Gondret. Local rheological measurements in the granular flow around an intruder. *Phys. Rev. E*, 93:012904, 2016.

[12] Andreea Panaitescu, Xavier Clotet, and Arshad Kudrolli. Drag law for an intruder in granular sediments. *Phys. Rev. E*, 95:032901, Mar 2017.

[13] Wenting Kang, Yajie Feng, Caishan Liu, and Raphael Blumenfeld. Archimedes' law explains penetration of solids into granular media. *Nature Communications*, 9(1):1101, Mar 2018.

[14] T. Takahashi, Abram H. Clark, T. Majmudar, and L. Kondic. Granular response to impact: Topology of the force networks. *Phys. Rev. E*, 97:012906, 2018.

[15] A. Seguin. Hysteresis of the drag force of an intruder moving into a granular medium. *The European Physical Journal E*, 42(1):13, Jan 2019.

[16] Satoshi Takada and Hisao Hayakawa. Drag acting on an intruder in a three-dimensional granular environment. *Granular Matter*, 22(1):6, Nov 2019.

[17] Christoph Kloss, Christoph Goniva, Alice Hager, Stefan Amberger, and Stefan Pirker. Models, algorithms and validation for opensource DEM and CFD-DEM. *Progress in computational fluid dynamics*, 12(2-3):140–152, 2012.

[18] CFDEM project. https://www.cfdem.com/liggghtsr-open-source-discrete-element-method-particle-simulation-code.

[19] Danielle S. Bassett, Mason A. Porter, Nicholas F. Wymbs, Scott T. Grafton, Jean M. Carlson, and Peter J. Mucha. Robust detection of dynamic community structure in networks. *Chaos: An Interdisciplinary Journal of Nonlinear Science*, 23(1):013142, 2013.

[20] Vincent D Blondel, Jean-Loup Guillaume, Renaud Lambiotte, and Etienne Lefebvre. Fast unfolding of communities in large networks. *Journal of Statistical Mechanics: Theory and Experiment*, 2008(10):P10008, 2008.

[21] Lucas G.S. Jeub, Marya Bazzi, Inderjit S. Jutla, and Peter J. Mucha. A generalized Louvain method for community detection implemented in MATLAB. https://github.com/GenLouvain/GenLouvain, 2011–2019.

[22] Matthew Steen, Satoru Hayasaka, Karen Joyce, and Paul Laurienti. Assessing the consistency of community structure in complex networks. *Phys. Rev. E*, 84(1):016111–1 – 016111–13, 2011.